ELSEVIER

Journal of Nuclear Materials 273 (1999) 239–247

journal of nuclear materials

www.elsevier.nl/locate/jnucmat

Behavior of metallic fission products in uranium–plutonium mixed oxide fuel

I. Sato [a,*], H. Furuya [a], T. Arima [a], K. Idemitsu [a], K. Yamamoto [b]

[a] *Department of Nuclear Engineering, Faculty of Engineering, Kyushu University, 6-10-1 Hakozaki, Fukuoka 812-8581, Japan*

[b] *Power Reactor and Nuclear Fuel Development Corporation, O-arai Engineering Center, Higashi Ibaraki-gun, Narita-cho, Oarai-machi, Ibaraki-ken 311-1393, Japan*

Received 28 August 1998; accepted 19 February 1999

Abstract

Metallic fission products, ruthenium, rhodium, technetium, palladium, and molybdenum, exist in irradiated oxide fuels as metallic inclusions. In this work, the radial distributions of metallic inclusion constituents in the fuel specimen irradiated to a peak burnup of 7–13 at.% were observed with an electron probe microanalysis. Palladium concentration is high at the periphery in all the specimens. Molybdenum shows the same tendency for the 13 at.% burnup specimen. These results showed the significant difference between experimental data and calculations with ORIGEN-2 at such high burnups, which suggested that the migration of palladium and molybdenum was controlled mainly by diffusion of gaseous species containing each metal along the fuel temperature gradient.

PACS: 28.41; 28.50

1. Introduction

Fast breeder reactor (FBR) fuels are expected to be used to a very high burnup from the reason of cost performance. The target burnup will be 20 at.% FIMA [1]. In other words, one fifth of the fuel metal will change into fission products. In order to attain this target burnup, it is basically important to know the behavior of fission products in the fuel.

Molybdenum, ruthenium, rhodium, technetium and palladium are produced in mixed oxide fuels with high fission yields and remain to be undissolved in fuel to precipitate as metallic inclusions. These are called the white metal phase, which has been well known from the early time [2].

Molybdenum concentration in the metallic inclusions in a $(U_{0.7}Pu_{0.3})O_{2-x}$ fuel pin irradiated to 13 at.% peak burnup in JOYO was lower than the expected value, and that part of the molybdenum was released from the fuel pellet to the fuel-cladding gap [3]. Tourasse et al. reported existence of a molybdenum and cesium-rich phase, so-called 'JOG', at the fuel-cladding gap in high burnup $(U_{0.8}Pu_{0.2})O_{2-x}$ fuels [4]. On the other hand, in fuel used in high temperature gas-cooled reactors, palladium is known to migrate relatively easily through the fuel matrix to the silicon carbide layer [5].

As mentioned above, molybdenum and palladium migrate in different manners from those for the other constituent elements of metallic inclusion. These behaviors of molybdenum and palladium, however, are not understood well, and then must be evaluated with a number of post irradiation examination data of many fuels irradiated under various conditions. In our previous paper [3], the radial concentration profile was only from molybdenum results measured in the fuels irradiated to 13.3 and 11.7 at.%, but no data for other metallic inclusion constituent elements.

In this work, the concentration profiles of all constituent elements in the metallic inclusion of the fuels

* Corresponding author. Tel.: +81 92 642 3779; fax: +81 92 632 3800; e-mail: sato@nucl.kyushu-u.ac.jp

0022-3115/99/$ – see front matter
PII: S0022-3115(99)00071-9

irradiated to burnups from 7 to 13 at.% were measured by using an electron probe microanalysis (EPMA) technique, and were presented with the quantitative metallography. Moreover, the migration behaviors of molybdenum and palladium in fuel were discussed based on these data.

2. Experimental

The fuels examined in this work were irradiated to the burnup of 7 to 13 at.% in the experimental fast reactor, JOYO, of Power Reactor and Nuclear Fuel Development Corporation (PNC). The as-fabricated characteristics and the local irradiation conditions of the fuel specimens are listed in Table 1. Most of the specimens were taken from axially near-middle locations of each fuel pin except for H71042 and G35722 fuel pins. Modified 316 stainless steel (PNC316) [6] was used as the cladding tube material. Post irradiation examinations were performed in the fuels monitoring facility (FMF) of O-arai Engineering Center of PNC.

Photographs along the radial direction on the transverse section were taken for each specimen with an optical microscope at magnification of either 400 or 520. Metallic inclusions can be distinguished as white spots from the fuel matrix on the photographs. Area of each spot for specimens H71042, H71062, G35722 and G35751 was measured to evaluate the fraction of occupation area of the metallic inclusions over the cross section of specimens. The minimum radius of the metallic inclusion that can be measured using this method was about 0.2 μm. The details of this procedure were reported elsewhere [7].

EPMA technique was adopted for measuring the concentrations of molybdenum, ruthenium, rhodium, technetium and palladium in the metallic inclusions. The acceleration voltage and absorption current were set to 25 kV and 0.1 μA, respectively. Characteristic X-rays detected for quantitative analyses were L_α for molybdenum, ruthenium, rhodium and technetium, and L_β for palladium.

3. Results

3.1. Radial profile of metallic inclusion

The cross section of the specimens was divided into 20–30 sections of concentric circles at equal interval along the radial direction. The radial concentration profile of the metallic inclusion was determined by measuring the fraction of occupation area of the metallic inclusions in each section.

Fig. 1 shows the occupation fraction profile of specimens G35722 (burnup of 10.4 at.%), G35751 (13.3 at.%), H71042 (9.6 at.%) and H71062 (10.6 at.%) along the radial direction from the cladding inner surface to the center of fuel pellet. It can be seen that the occupation fraction profiles depend on the burnup or linear heat rating. On the highest burnup specimen, G35751, the fraction of occupation area of the metallic inclusions reached a peak at about 700 μm from the cladding inner surface, while it does at 1000 μm on H71062 also. In the specimens, H71042 and G35722, irradiated to relatively low burnups at lower linear heat ratings, however, the radial profiles were flat compared with the ones of G35751 and H71062. From the difference in the profiles between the fuels irradiated to relatively high and low burnups, it is suggested that the metallic inclusion migrates over a considerably large distance in the higher burnup fuel, considering that the FBR fuel has little neutron depression.

Table 1
As-fabricated characteristic and irradiation condition of fuel specimens

Pin no.	Specimen no.	Fractional location from fuel column bottom	As-fabricated characteristics				Local irradiation condition		
			Pu/(Pu+U)	Density (%TD)	O/M ratio	Diameter (mm)	Linear heat rating at EOL (kW/m)	Burnup (at.%)	Cladding inner surface temperature at EOL (K)
A429	A42944	0.45	0.299	85	1.94	5.4	28.8	6.8	809
C860	C86062	0.45	0.293	93	1.97	4.6	23.4	9.6	753
C7A6	C7A662	0.455	0.293	93	1.97	4.6	24.0	7.6	758
	H71042	0.23					22.2	9.6	716
H710			0.300	85	1.95	5.4			
	H71062	0.46					24.2	10.6	762
G305	G30561	0.51	0.297	85	1.95	5.4	25.8	11.9	765
	G35722	0.07					20.9	10.4	695
G357			0.298	85	1.94	5.4			
	G35751	0.50					26.4	13.3	791

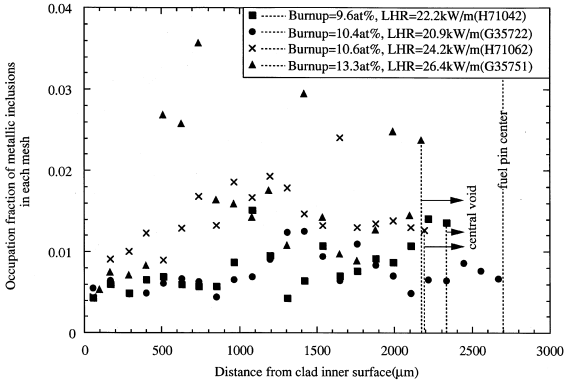

Fig. 1. Fraction of occupation area of metallic inclusions in each section as a function of distance from cladding inner surface of each specimen fuel matrix.

3.2. Concentration profiles of the constituent elements in the metallic inclusions

Figs. 2–4 show the profiles of relative concentrations (fractions) of constituent elements, molybdenum, ruthenium, rhodium, technetium and palladium, in the metallic inclusion as a function of distance from the cladding inner surface each for A42944 (6.8 at.% burnup), H71062 (10.6 at.% burnup) and G35751 (13.3 at.% burnup), respectively. In Figs. 3 and 4, five kinds of lines represent the relative concentrations calculated by ORIGEN-2 code with reasonable the assumption that the neutron flux is radially flat in the fuel.

Comparison of Figs. 2 and 3 indicates that the palladium migrates toward the outer fuel surface and that the amount of palladium migration increases with burnup. For the highest burnup specimen, it can be seen in Fig. 4 that the relative concentrations of molybdenum

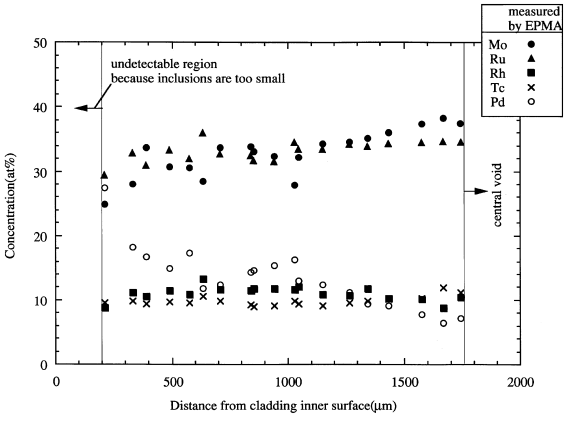

Fig. 2. Concentration profiles of molybdenum, ruthenium, rhodium, technetium and palladium in metallic inclusions (burnup = 6.8 at.%, A42944).

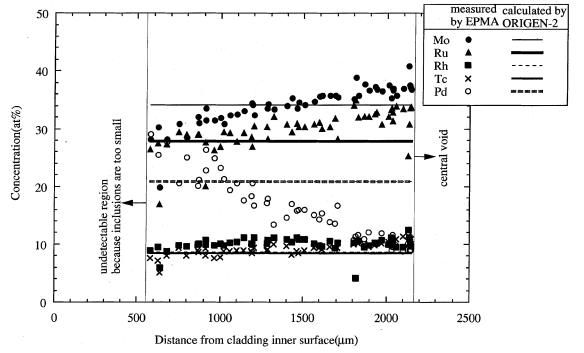

Fig. 3. Concentration profiles of molybdenum, ruthenium, rhodium, technetium and palladium in metallic inclusions (burnup = 10.6 at.%, H71062).

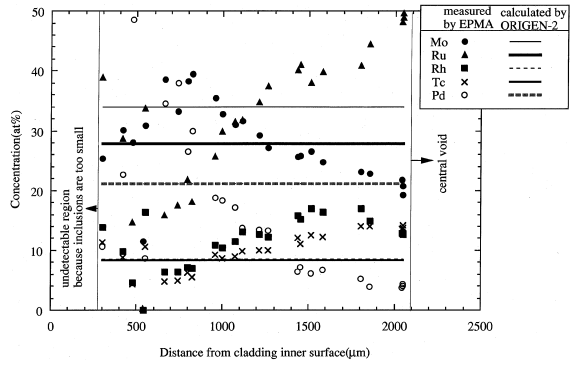

Fig. 4. Concentration profiles of molybdenum, ruthenium, rhodium, technetium and palladium in metallic inclusions (burnup = 13.3 at.%, G35751).

and palladium have peaks around 700 μm from the inner surface of cladding, where the fraction of occupation area of metallic inclusion is highest as shown in Fig. 1.

The concentrations of ruthenium, rhodium and technetium increase toward the fuel center, but the possibility of migration of these elements is little since these changes can be expected from the decrease of concentrations of molybdenum and palladium near the center.

3.3. Appearance of large metallic inclusion

The size of the metallic inclusions was 10 μm generally. Large metallic inclusions can be observed near the outer fuel surface. Fig. 5 shows a photograph of such a typical large precipitate observed in the specimen H71042. This precipitate has higher concentrations of palladium and ruthenium than the usual precipitates, and accompanies the barium oxide phase and void in the adjacent region.

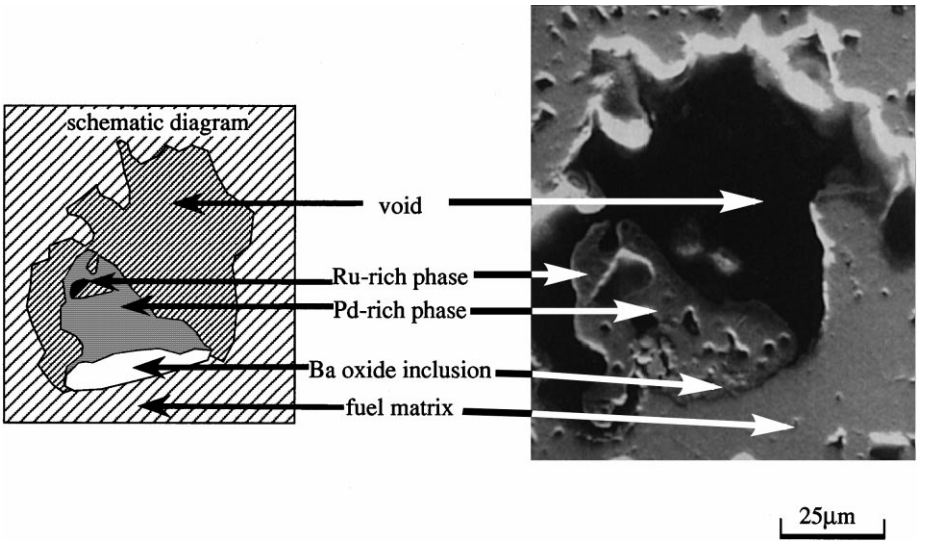

Fig. 5. A metallic inclusion consisting mainly of palladium located near fuel periphery (burnup = 9.6 at.%, H71042).

4. Discussion

4.1. Concentration profiles of palladium and molybdenum

The rare metal elements which have little solubility in the fuel matrix precipitate, and subsequently form the metallic inclusions in the grains or grain boundaries. The migration of constituent elements in the metallic inclusions along the temperature gradient in fuel includes two processes. One is the migration accompanied by the fuel restructuring, which takes place mainly in the early stage of irradiation. Another is the vaporization–condensation through the cracks and tunnels formed by the connection of fission gas bubbles on the grain boundary. The difference in the extent of migration among the constituent elements makes the concentration profile uneven. In this work, the following discussions are focused on the latter process, because the specimens were irradiated to high burnup.

The EPMA observations shown in Figs. 2–4 indicate that the migration of palladium from the fuel center to the periphery begins at relatively low burnup, while that of molybdenum does at high burnup. In contrast, the relative concentrations of ruthenium, rhodium and technetium in the metallic inclusions increase preferentially along the direction to the fuel center. However, for these elements, the actual migration may be of a lesser extent, because the gradual increase of palladium and molybdenum concentrations toward the fuel periphery should entail the gradual decrease in the relative concentrations.

Fig. 6 shows the concentration ratio of molybdenum to ruthenium (called as Mo/Ru ratio here) and palladium concentration in the metallic inclusions close to the central void as a function of burnup, together with Tourasse's result of Mo/Ru ratio [4]. The shaded areas show the regions expected from the calculation by using ORIGEN-2 code. This figure suggests that palladium moves even at a low burnup, while molybdenum begins to migrate over 10 at.%. The present result for Mo/Ru ratio is higher than Tourasse's result. The observed difference may be attributed to the difference in the irradiation conditions (especially linear heat rating) and fuel characteristics (especially O/M ratio) between the studies.

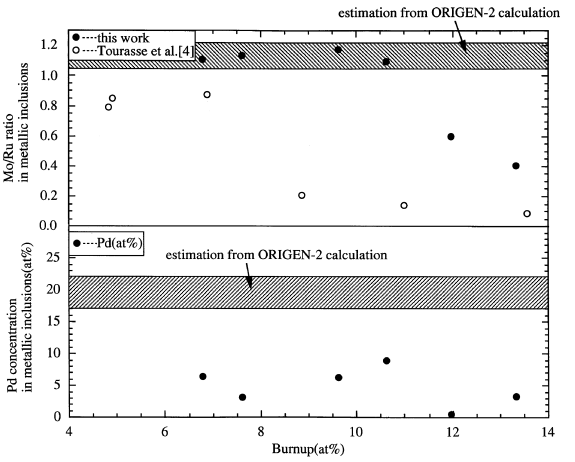

Fig. 6. Burnup-dependence of Mo/Ru concentration ratio and Pd concentration in metallic inclusions near the central void.

The compositions of metallic inclusions obtained in this work are tentatively plotted in the quasi-ternary molybdenum–(ruthenium, technetium)–(palladium,

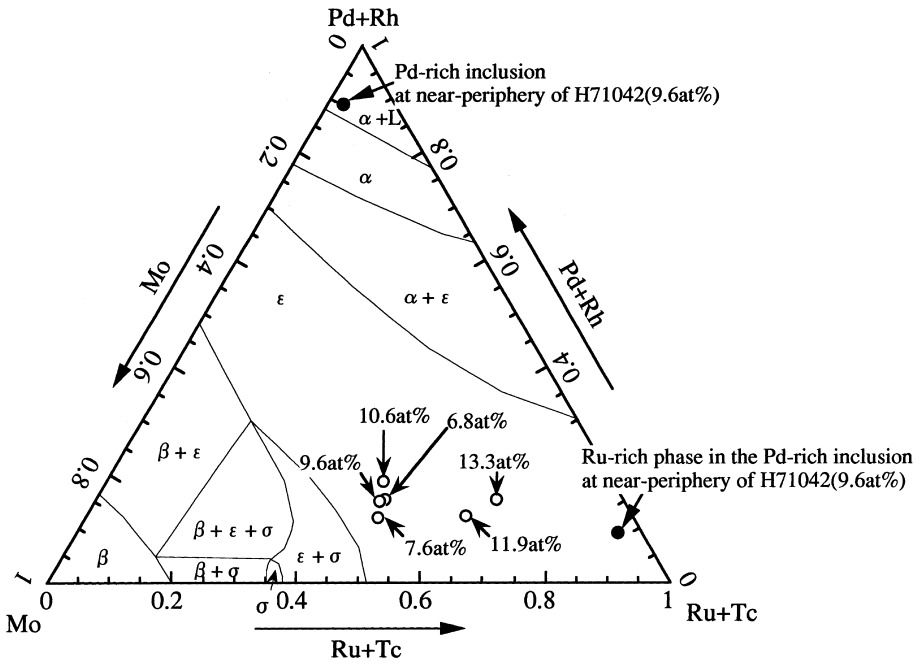

Fig. 7. Quasi-ternary Mo–(Tc, Ru)–(Pd, Rh) phase diagram [9] at 1700°C with this work data near central voids (○) and near periphery (●).

rhodium) phase diagram given by Kleykamp [8] for 1700°C as shown in Fig. 7, although this temperature does not agree with the temperature of the fuel during irradiation. In Fig. 7, open symbols indicate compositions of inclusions near the central void for 6.8 at.% (A42944), 9.6 at.% (C86062), 7.6 at.% (C7A662), 10.6 at.% (H71062), 11.9 at.% (G30561) and 13.3 at.% (G35751). In addition, solid symbols do compositions of two phases in the large metallic inclusion of H71042 (9.6 at.% burnup) shown in Fig. 5.

From this phase diagram, it can be seen that the compositions of all inclusions remain in the single ε-phase region except one of H71042, and that the compositions of ones in the fuel irradiated to a higher burnup (11.9 and 13.3 at.%) shift to ruthenium- and technetium-rich regions. The inclusions in high burnup fuels are poor in molybdenum, compared with other ones. The large inclusion formed near the periphery of H71042 at relatively low temperature consists mainly of palladium which migrated from the higher temperature region. It is most likely that a large amount of palladium segregates ruthenium in the metallic inclusion to form a small volume of ruthenium rich phase.

4.2. Migration mechanisms of palladium and molybdenum

Fission gases mainly release easily through some paths, such as macro- or micro-cracks, grain boundaries and interconnected tunnels [9]. Migrations of palladium and molybdenum by means of gaseous molecules diffusion through these paths [10] can be assumed to be an operative mechanism, because molybdenum and palladium are expected to migrate substantially and easily as much as fission gases according to the observations and considerations mentioned above.

First, discussion will be focused on the migration mechanism of palladium which can not form an oxide under the oxygen potentials expected to be attained in the FBR oxide fuel during irradiation. Some couples of researchers have measured and calculated either the vapor pressures or the activities of constituent elements in several kinds of metallic inclusions over the temperature range at 1000–2000 K [11–14]. According to their investigations, the degree of vapor pressures of constituent elements changes in a descending order of palladium, rhodium, ruthenium and molybdenum under vacuum. For instance, the vapor pressure of palladium and rhodium are 10^{-8} and 10^{-15} Pa at 1000 K, and 10^{-2} and 10^{-6} Pa at 1500 K, respectively.

By assuming that vapors with higher pressures contribute more toward the radial migration, the experimental results shown in Figs. 2–4 can be well understood, i.e. palladium begins to migrate at a burnup less than 10 at.%, and has more than 10^{-2} Pa of the vapor pressure around the central void. The vapor pressure of the solid can be expressed such as

$A\exp(-\Delta H/RT)$ and so has a strong temperature dependence, while there is little dependence of palladium vapor pressure on its composition of alloys [13,14]. It is expected that palladium migrates by means of gaseous molecules diffusion along the vapor pressure gradient created by temperature gradient in fuels.

Next, migration of gaseous molecules containing molybdenum, of which metallic vapor pressure over pure metal is the lowest in all the constituent elements, is discussed. It is well-known that the molybdenum, unlike palladium, forms several kinds of chemical compounds, depending on the oxygen partial pressure. Matzke et al. reported the burnup-dependence of oxygen partial pressure and showed that the partial pressure of $(U_{0.8}Pu_{0.2})O_{1.98}$ could change from 10^{-13} to 10^{-7} Pa at 1500 K with the increase of the burnup up to 11.2 at.% [15]. At the higher temperatures, the oxygen partial pressure was higher than 10^{-7} Pa.

In order to evaluate gaseous migration of molybdenum, the chemical forms of molybdenum were considered in the range of oxygen partial pressure in FBR oxide fuel during irradiation. Mo, MoO_2, Cs_2MoO_4 and MoO_3 are found as gaseous molybdenum-containing species. Cs_2MoO_4 can form more easily than others since its free energy of formation is the lowest. However, according to EPMA observations, cesium remaining in the higher temperature region was significantly low because of high mobility of elemental cesium and other cesium compounds [16]. Therefore, Cs_2MoO_4 may not contribute to the migration of molybdenum in a high burnup fuel.

Matsui et al. estimated vapor pressures of the species containing molybdenum as a function of oxygen partial pressure over $Mo_{0.45}Ru_{0.45}Pd_{0.1}$ alloy based on the regular solution model [11]. The vapor pressure of $(MoO_3)_3$ was highest beyond the oxygen partial pressure of 10^{-7} Pa, which was expected to be equivalent to the one in high burnup fuels. Here, $(MoO_3)_3$ is a polymeric molybdenum oxide. MoO_3 tends to be some polymeric states in gas phase [17]. Over 10^{-7} Pa of the oxygen partial pressure, the vapor pressure of $(MoO_3)_3$ is 10^{-3} Pa, and is comparable with the vapor pressure of palladium, 10^{-2} Pa at 1500 K. In their work, pressures of vapors containing either of the other constituent elements were estimated over molybdenum–ruthenium–palladium, molybdenum–ruthenium–rhodium and molybdenum–technetium–palladium alloys, and their vapor pressures were lower than the vapor pressures of MoO_3 and $(MoO_3)_3$ in the interesting range of oxygen partial pressure. These suggest that molybdenum can migrate as gaseous species $(MoO_3)_3$ or MoO_3, at high oxygen potential, which corresponds to the oxygen pressure of the fuel irradiated to a high burnup.

4.3. An attempt of quantitative analysis on the migration of palladium along the temperature gradient

The EPMA observation showed that palladium migrated from the center of fuel at high temperature to the periphery of fuel at low temperature, which indicated that palladium migrated as gaseous species, resulting from the difference in vapor pressure. In order to explain this result, the migration mechanism of palladium is discussed here on the basis of the diffusive or convection transports [18–20]. The Fick's first law of diffusion is employed to confirm whether the palladium vapor emitted from the metallic phase could diffuse along the temperature gradient. This method was advocated by Watanabe et al. [18]. It is assumed that there exist only the metallic vapors in the considered system, so that the gaseous oxide species such as $(MoO_3)_3$ are neglected.

The deposition–vaporization rate, R_{Me}, of each metallic element, which indicates its degree, can be expressed in Eq. (1). This equation was obtained through the derivation shown in Appendix that had been performed based on the literature [16,18,21–27].

$$R_{Me} = \frac{5.082\times10^{-9}}{\sqrt{M_{Me}}}\times 10^{(A_{Me}+B_{Me}/T)}(\alpha+\beta+\gamma)\quad (\mathrm{mol/m^3\ s}), \tag{1}$$

where

$$\alpha = B_{Me}(\ln 10)\left(\frac{dT}{dx}\right)^2 \times (B_{Me}(\ln 10)T^{-4.5}+T^{-3.5}),$$

$$\beta = -\frac{d^2T}{dx^2}(B_{Me}(\ln 10)T^{-2.5}+T^{-1.5}),$$

$$\gamma = \left(\frac{dT}{dx}\right)^2\left(2.5B_{Me}(\ln 10)T^{-3.5}+1.5T^{-2.5}\right).$$

Me, M_{Me} and T are an element of the metallic inclusion, the atomic weight (kg/mol) of Me and absolute temperature, respectively. The vapor pressure of Me changes as a function of temperature according to the equation $10^{(A_{Me}+B_{Me}/T)}$, where A_{Me} and B_{Me} are constants for Me. Eq. (1) shows that the deposition–vaporization rate is proportional to the vapor pressure.

The deposition–vaporization rate of each constituent element was estimated by applying Eq. (1) to an imaginary system, where there is a temperature gradient such as along the fuel radius. The system is a tube of which the inner surface is homogeneously covered with the metallic elements. The metallic gaseous molecules can axially move in the tube system. To make an estimation of such a system requires to determine the axial temperature distribution and the constants A_{Me} and B_{Me}. The former was acquired for a specimen, G35751, with a code for thermal and deformation analysis of reactor

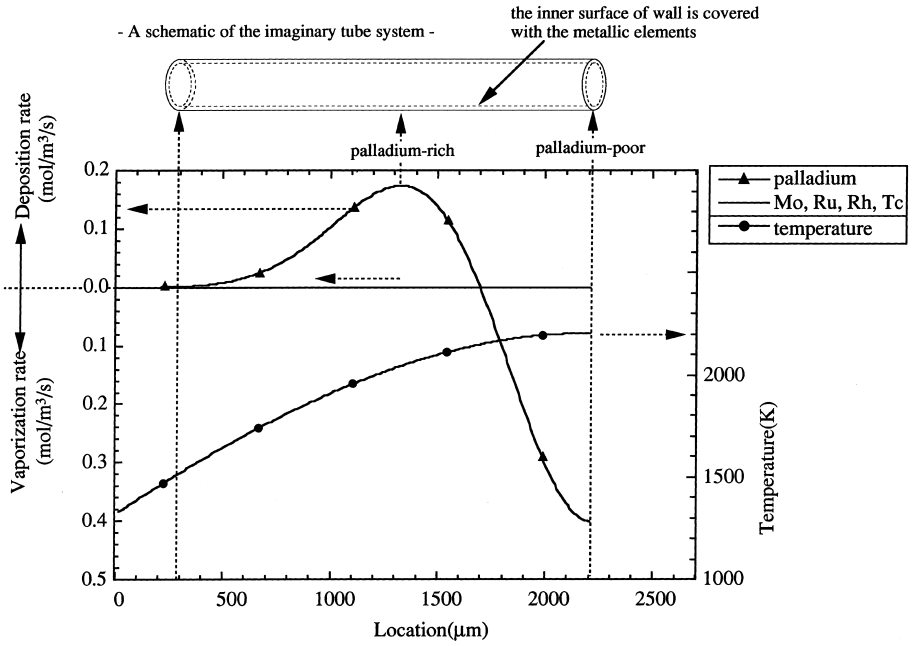

Fig. 8. Deposition–vaporization rate of the metallic elements and the temperature distribution over the imaginary tube system.

fuel, CEDAR [28]. The latter was obtained from experimental data [23–27] over each pure metal in vacuum.

Fig. 8 shows the deposition–vaporization rates for five constituent elements as a function of location. This figure illustrates that palladium can be removed from the hotter region and deposit at the colder one. And the magnitudes of deposition and vaporization rates of other elements are much smaller than that of palladium since palladium has higher vapor pressures by four orders of magnitude compared to the other elements.

The deposition-vaporization rate profile agrees with the concentration profile obtained in the EPMA observations. It is well understood that only palladium can migrate preferentially from the hotter region to the colder one. However, the calculation and the EPMA observation for the concentration profile show a peak at the middle and at the periphery of the fuel pellet, respectively. This disagreement probably arises from a difference of path cross sections between the imaginary and the real fuel systems. In other words, the real paths of gaseous metals are heterogeneously distributed in the irradiated fuel system, and not similar to the tube assumed in the imaginary system. Better models of the path for gaseous migration are needed in order to grasp the migration of palladium in the form of gaseous species in detail.

5. Conclusion

The migrations of palladium and molybdenum were evaluated on the basis of the quantitative metallography and concentration profiles of constituent elements in the metallic inclusion of FBR mixed oxide fuels irradiated to 7–13 at.%, together with the results of thermodynamic and kinetic analyses. The findings are summarized as follows:

(1) Palladium migrates from the center to periphery of fuel along a temperature gradient at low burnup.

(2) Molybdenum begins to migrate at over 10 at.% burnup.

(3) Palladium can migrate as a gaseous metal, while molybdenum can do as $(MoO_3)_3$ or MoO_3 in high oxygen potential.

(4) Such migrations for gaseous species may depend on the actual configuration of the paths formed in the fuel during irradiation.

Acknowledgements

The authors are grateful to Mr Y. Ohsato, Mr Y. Onuma and Mr S. Nukaga (Nuclear Technology & Engineering Corporation) for help in the experiments.

Appendix A

The diffusion coefficients of molybdenum, ruthenium, rhodium, technetium and palladium are estimated in gas phase of fuel during irradiation as follows. There are fission gases, volatile fission product gases and the

inert gas in the fuel, but it is assumed in this calculation that only xenon and vapors of the constituent elements of metallic inclusion fill in the system because of higher fission yield of xenon than other gaseous FPs. The theoretical diffusion coefficient of each constituent element is [21]

$$D_{\mathrm{Me}} = \frac{1}{6}\lambda_{\mathrm{Me}}^2 \Gamma_{\mathrm{Me}}, \tag{A1}$$

where $\lambda_{\mathrm{Me}} = 1/(\sqrt{2}\pi/V)\sum_i (N_i d_i^2)$ (the mean free path of Me),

$$\Gamma_{\mathrm{Me}} = \sqrt{\frac{8RT}{\pi M_{\mathrm{Me}}}}\ (\text{collision frequency of Me}).$$

The symbols of Me, D_{Me} and M_{Me} are an element of the metallic inclusion, the diffusion coefficient (m^2/s) of Me and the atomic weight (kg/mol) of Me, respectively. The symbol N_i, d_i, V, T and R are number of i element in the system, atomic radius (m) of i, system volume (m^3), temperature (K) and gas constant (J/mol/K). $\sum(N_i d_i^2)$ mainly depends on N_{xenon}, because the pressure of xenon is higher by five orders of magnitude than the other gases. N_{xenon}/V is proportional to the pressure in the system. The pressure of the xenon is about 15.6 atm at room temperature according to the pin puncture test of G357 pin [16], then

$$D_{\mathrm{Me}} = 4.223 \times 10^{-8}\sqrt{\frac{T}{M_{\mathrm{Me}}}}\ (\mathrm{m}^2/\mathrm{s}). \tag{A2}$$

The diffusion coefficients depend only on temperature because the weight of each element is almost equal to one another.

According to the first diffusion law of Fick, the flux, J_{Me}, of Me through the gas phase is

$$J_{\mathrm{Me}} = -D_{\mathrm{Me}}\Delta C_{\mathrm{Me}} = -D_{\mathrm{Me}}\frac{\mathrm{d}C_{\mathrm{Me}}}{\mathrm{d}x}, \tag{A3}$$

where C_{Me} (mol/m^3) and x are the concentration of Me in the gas phase and the location. By the use of Boyle–Charles' law, C_{Me} is expressed as follows [18]:

$$C_{\mathrm{Me}} = \frac{N_{\mathrm{Me}}}{V} = \frac{P_{\mathrm{Me}}}{RT}. \tag{A4}$$

Moreover, a temperature dependence of the vapor pressure over each solid metal is [22]

$$P_{\mathrm{Me}} = 10^{(A_{\mathrm{Me}} + B_{\mathrm{Me}}/T)}. \tag{A5}$$

A_{Me} and B_{Me} can be determined from some experimental data such as Refs. [23–27]. Substituting Eq. (A2), Eq. (A4) and Eq. (A5) into Eq. (A3),

$$J_{\mathrm{Me}} = \frac{5.082 \times 10^{-9}}{\sqrt{M_{\mathrm{Me}}}} \times 10^{(A_{\mathrm{Me}} + B_{\mathrm{Me}}/T)} \times \frac{\mathrm{d}T}{\mathrm{d}x}\left\{\frac{B_{\mathrm{Me}}(\ln 10)}{T^{2.5}} + T^{-1.5}\right\}. \tag{A6}$$

In steady state, the deposition–vaporization rate [18] is a differential of the flux for the location, x; therefore

$$R_{\mathrm{Me}} = \frac{-\mathrm{d}J_{\mathrm{Me}}}{\mathrm{d}x}. \tag{A7}$$

References

[1] M. Hori, T. Fukuda, T. Takahashi, Proceedings of the International Conference on Fast Reactor and Related Fuel Cycle (FR '91), Kyoto, Japan, October 28–November 1, 1991, vol. 1, pp. 1–5.
[2] D.R. Olander, Fundamental aspects of nuclear reactor fuel elements, TID-26711-P1, T.I.C., 1976.
[3] I. Sato, H. Furuya, K. Idemitsu, T. Arima, K. Yamamoto, M. Kajitani, J. Nucl. Mater. 247 (1997) 46.
[4] M. Tourasse, M. Boidron, B. Pasquet, J. Nucl. Mater. 188 (1992) 49.
[5] K. Minato, T. Ogawa, S. Kashimura, K. Fukuda, M. Shimizu, Y. Tayama, I. Takahashi, J. Nucl. Mater. 172 (1990) 184.
[6] I. Shibahara, S. Ukai, S. Onose, S. Shikakura, J. Nucl. Mater. 204 (1993) 131.
[7] I. Sato, T. Arima, H. Furuya, K. Yamamoto, K. Konno, M. Kajitani, PNC TY9606 97-001 (in Japanese).
[8] H. Kleykamp, Nucl. Tech. 80 (1988) 412.
[9] R.J. White, M.O. Tucker, J. Nucl. Mater. 118 (1983) 1.
[10] H. Kleykamp, J. Nucl. Mater. 131 (1985) 221.
[11] T. Matsui, K. Naito, J. Nucl. Sci. Tech. 26 (1989) 1102.
[12] M. Yamawaki, Y. Nagai, T. Kogai, M. Kanno, Thermodynamics of Nuclear Materials, IAEA, Vienna 1 (1980) 249.
[13] K. Naito, T. Tsuji, T. Matsui, A. Date, J. Nucl. Mater. 154 (1988) 3.
[14] T. Matsui, K. Naito, Thermochim. Acta 139 (1989) 299.
[15] Hj. Matzke, J. Ottaviani, D. Pellottero, J. Rouault, J. Nucl. Mater. 160 (1988) 142.
[16] private communication (1996).
[17] J. Berkowitz, M.G. Ingraham, W.A. Chupka, J. Chem. Phys. 26 (1957) 842.
[18] H. Watanabe, T. Nishinaga, T. Arizumi, J. Cryst. Growth 17 (1972) 183.
[19] H. Schafer, J. Cryst. Growth 9 (1971) 17.
[20] R.F. Lever, G. Mandel, J. Phys. Chem. Solids 23 (1962) 599.
[21] M. Yoneyama, S. Sato, H. Ohashi, T. Ogawa, A. Ito, J. Nucl. Mater. 247 (1997) 50.
[22] W.J. Moore, Physical Chemistry, 4th Ed., Prentice-Hall, New Jersey, 1972.
[23] D.R. Stull, H. Prophet, JANAF Thermochemical Tables, 2nd Ed., p. 967, 970–977.
[24] N.J. Carrera, R.F. Walker, E.R. Plante, J. Res. NBS 68A (1964) 325.

[25] R.F. Hampson, R.F. Walker, J. Res. NBS 65A (1961) 289.
[26] H.L. Schick, Thermodynamic of Certain Refractory Compounds, Academic Press, New York, 1966, p. 1390.
[27] J.V. Panesko, ARH-1552, 1971.
[28] T. Mizuno, S. Nagai, T. Itaki, N. Nagae, K. Tanaka, J. Komatsu, Proceedings of the International Conference on Reliable Fuels for Liquid Metal Reactors, Tucson, Arizona, 1986, pp. 5–28.